DENTAL MATERIALS 37 (2021) 1425–1436

Available online at www.sciencedirect.com

ScienceDirect

journal homepage: www.intl.elsevierhealth.com/journals/dema

Pre-cementation procedures' effect on dental zirconias with different yttria content

Marit Øilo[a,b,*], Ketil Haugli[a,c], Hans Jacob Rønold[a,d], Amanda H. Ulsund[d], Amund Ruud[a], Ketil Kvam[a]

[a] NIOM, Nordic Institute of Dental Materials, Oslo, Norway
[b] Department of Clinical Dentistry, Faculty of Medicine, University of Bergen, Bergen, Norway
[c] OSLOMET, Oslo Metropolitan University, Oslo, Norway
[d] Department of Clinical Dentistry, Faculty of Dentistry, University of Oslo, Oslo, Norway

ARTICLE INFO

Article history:
Received 16 November 2020
Received in revised form
26 April 2021
Accepted 7 July 2021

Keywords:
Dental ceramics
Luting agents
Surface modification
Fractography
Zirconuim dioxide

ABSTRACT

Objective. Several pre-cementation procedures have been advocated to enhance adhesion between zirconia and resin-based cement. There is, however, limited documentation on how these pre-treatments affect the strength of zirconia crowns as most tests are performed on discs or bars.

The aim was to assess the effect of pre-cementation procedures on fracture mode, fracture strength and cement retention on zirconia.

Methods. Two dental zirconia materials with different yttria content were assessed (<4 and>5 mol%). Both discs (n = 45) and crown-shaped specimens (n = 30) of the two materials were pretreated with either air-abrasion or hot-etching with KHF_2 and compared with untreated controls with regards to surface roughness, crystallography, wettability, cement adhesion and fracture strength.

Results and Significance. Air-abrasion improves adhesion and strength of zirconia with moderate yttria content (<4 mol%). Acid etching with heated KHF_2 showed the best effect on strength and cement retention on zirconia with higher yttria content (>5 mol%). Application of KHF_2 was, however, complicated on crown-shaped specimens. Pre-treatment and cementation protocols should be optimized for different dental zirconias to improve both strength and retention.

1. Introduction

Since the introduction of yttria-stabilized tetragonal zirconia polycrystal (Y-TZP) for fixed dental restorations, attempts have been made to improve adhesive bonding to the restorations' intaglio surface in order to enhance retention [1–5]. Loss of retention and fractures are the main reasons for failure of zirconia restorations. Several different methods show promising results when tested *in vitro*, but only a few clinical studies are published so far [6,7]. The recommendations from manufacturers vary likewise, making it challenging for the dental technicians and dentists to decide on the optimal treatment of the restorations for cementation.

Air-borne particle abrasion (air-abrasion) with Al_2O_3 particles is one of the most used and tested methods, and

* *Corresponding author at*: Department of Clinical Dentistry, Arstadveien 19, 5009 Bergen, Norway.
E-mail address: marit.oilo@uib.no (M. Øilo).

https://doi.org/10.1016/j.dental.2021.07.001

often recommended by manufacturers [5,7,8]. The particle size and pressure vary among the different studies, but recent studies indicate that 1.5–2 bar pressure and ≈50 μm particle size gives a surface roughness that is sufficient to increase retention compared to untreated surfaces [7,9]. Etching with phosphoric (H_3PO_4) or hydrofluoric (HF) acid has been evaluated in several studies, but with limited evidence of increased retention [10–12]. A recent trial suggests that surface treatment with potassium hydrogen difluoride (KHF_2) at 280 °C, improves retention [13,14]. There is limited knowledge regarding how either of these treatments affects material strength.

Most studies assessing the strength of adhesion between zirconia and a resin cement are performed as micro tensile tests, shear bond strength tests or similar, simplified *in vitro* tests. [15]. The effects of surface treatment on the strength of the zirconia are rarely addressed [16,17]. It has, however, been shown that too rough surface treatment can weaken zirconia restorations both in the short and long term [16]. Flat specimens (discs or bars) are most commonly used when assessing different surface treatments, making it easy to assess different treatments in a standardized manner. The more complex shape of the restorations can make it challenging to transfer these initial surface treatments to the actual restoration [18]. For example, it is difficult to uniformly air-abrade the inside of a crown at a standardized distance and a certain angle. Furthermore, applying liquids inside crowns with walls of variable height is virtually impossible without spilling. The complex geometry of prosthetic restorations may affect how stress fields develop during loading [19]. It is thus uncertain whether the results from in *vitro trials* of discs can be directly transferred to clinical restorations.

Recently, zirconia with increased amount of yttria-stabilizer (>5 mol%) has been introduced as an ultra-translucent dental restorative material with partial or full cubic (*c*) phase stabilization sometimes called partially stabilized zirconia (PSZ) and fully stabilized zirconia (FSZ) [9,20,21]. The terminology is not well established within dental literature and the terms 5Y-TZP or 8Y-TZP are sometimes used as well, although the material is not stabilized in the tetragonal phase (*t*). The terms 3Y, 5Y and 8Y zirconia probably give a more relevant presentation of the materials, with the numbers indicating the doping levels of yttria in zirconia in mol%. Within dentistry, increasing yttria amounts are associated with an increase in translucency but with a reduction in strength. It is uncertain whether the cementation procedures should be similar for all types of zirconias [9].

The aim of this study was to assess the applicability and effect of two different pre-cementation procedures, and whether these pre-treatments affect load at fracture, fracture modes, surface structure, surface energy and cement retention on dental zirconia with 3 and 5 mol% yttria. Both crown- and disc-shaped specimens were used in order to evaluate whether the use of simplified *in vitro* test methods is sufficient to assess the effect of pre-treatment for clinical restoration.

The null hypothesis was that pre-cementation procedures do not affect load at fracture, fracture mode, surface structure, surface energy or cement retention, and no differences can be found between discs- and crown-shaped specimens or between 3Y and 5Y zirconia.

2. Materials and methods

Two commercially available dental zirconias intended for single crowns and fixed partial dentures were tested (Table 1). One with multiple indications for fixed prosthodontics with 3–4 mol% yttria-stabilizer (3Y-Z) and one with higher translucency intended for anterior restorations with >5 mol% yttria-stabilizer (5Y-Z). Disc- and crown-shaped specimens were made of both materials for comparison between clinical scenario and optimal laboratory setting.

2.1. Crowns

Thirty crowns of each material were produced to fit a shallow chamfer preparation (Fig. 1) on an artificial canine tooth (KAVO Dental, Biberach, Germany). The specimens were digitally designed and saved as STL-files prior to importation of the files in corresponding design software (Fräsen ver. 4003_0030, Zirkonzahn, Gais, Italy) for the milling unit (M1 Wet Heavy Metal Milling Unit, ZirkonZahn, Gais, Italy). After milling, the connectors holding the specimens in place, were carefully separated with a diamond burr at 7000 rpm.

2.2. Discs

Cylinders were milled from partially pre-sintered blocks and forty-five slices were cut from these with an Accutom cutting machine with a diamond cutting wheel (Struers, Ballerup, Denmark). The slices were ground with 500 grit SiC paper to dimensions and parallelism (with the expected shrinkage during final sintering taken into account) of the flat surfaces following ISO 6872:2015. The sintered discs were ground at one surface with a diamond disc (Dac, diamonds with 20 μm grain size, Struers, Ballerup, Denmark) to enhance parallelism and provide a flat surface for the loading piston on the compressive side.

2.3. Sintering

A clean and soft porcelain brush and compressed air were used to remove excess zirconia dust after the milling process. All specimens, both discs and crowns, were subsequently sintered in a furnace programmed for the two materials (Zirkonofen 700, Zirkonzahn, Gais, Italy).

2.4. Pre-cementation surface treatment

The specimens from each material were randomly allocated into three groups. The test surfaces were left untreated for one group, as controls, one group was hot acid-etched, and the last group was air-abraded with alumina particles. All specimens were subsequently steamed and ultrasonically cleaned in ethanol for 15 min before, steamed again and blown dry with compressed air.

2.4.1. Air borne particle abrasion

The specimens were air-abraded at 2.5 bar for 10 s with 50 μm alumina (Al_2O_3) particles. The nozzle was kept perpendicular to the test surfaces of the discs and as perpendicular as possi-

Table 1 – The materials used in the study for both discs and crowns with material names, composition (provided by producer), sintering temperature and producer information.

Abbrev	Material name	Composition (weight%/mol%)	Sintering temperature	Producer name, city, country
3Y-Z	Prettau Zirkon	ZrO_2 – main component Y_2O_3 – 4–6%/2.22–3.37% Al_2O_3 – max 1% SiO_2, Fe_2O_3, Na_2O < 0.04%	Heating: 6 °C/ min. to 1.600 °C. Holding time at max. temp: 120 min. Cooling: 6 °C/min. to room temp.	ZirkonZahn, Gais, Italy
5Y-Z	Prettau Anterior	ZrO_2 – main component Y_2O_3 –12%/6.93% (max) Al_2O_3 – max 1% SiO_2, Fe_2O_3 < 0.02%	Heating: 8 °C/ min. to 1.500 °C. Holding time at max. temp:120 min. Cooling: 8 °C/min. to room temp.	ZirkonZahn, Gais, Italy

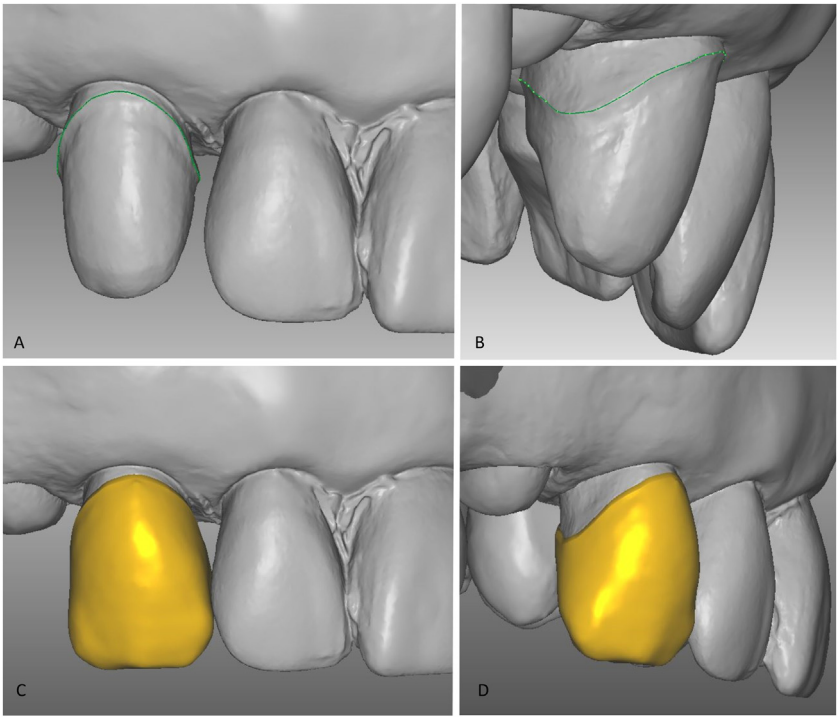

Fig. 1 – A shallow chamfer preparation on an artificial upper canine. Buccal (A) and distal (B) view of the prepared tooth, the crown was designed with a flattened incisal edge. Buccal (C) and distal (D) view of the designed crown.

ble to the intaglio surfaces of the crowns (angle between 60 to 90°) at 10 mm distance. The air-abrasion was performed with sweeping circular motions to ensure even application.

2.4.2. *Hot etching procedure*

KHF_2 crystals were ground to a fine powder with a pestle and mortar and applied equally on the bonding surface of the zirconia specimens [13]. Care was taken to fill the crowns completely by packing the powder towards the protruding buccal and lingual flange. After that, the specimens were heated in a pre-calibrated furnace (Jelenko, Accu-therm II 2000, NY, USA) for 10 min at 280 °C for the KHF_2 to melt. After cooling, the specimens were rinsed in running water.

2.5. *Assessment of surface quality*

After surface treatments, contact angle measurements were performed on the disc-shaped specimens (NRL Contact angle goniometer, Ramé-hart instrument co.). The three-point contact angle at the solid–liquid–gas interface gives a measure of the wettability of the solid material by the liquid. The surface energy was evaluated by using deionized distilled water on ten random specimens in each test group and five random specimens from each test group were tested with bonding liquid (Clearfil Universal Bond Quick Kuraray Noritake Dental Inc. LOT: 7L0040). A scaled micropipette was used to produce a drop of 0.01 (±0,003) gram of deionized water which was carefully deposited from the same distance

on the ceramic-surface (as close to the surface as possible). The contact angle was measured within 10 s after the droplet settlement. The bonding was transferred from the bottle to a micropipette for dispensing an identical amount each time.

Sample surfaces were investigated with scanning electron microscopy (SEM, TM4000Plus SEM, Hitachi, Japan). Both a semiconductor backscattered electron (BSE) detector and a secondary electron (SE) detector were used for analyses of the surfaces. The further surface evaluation was performed with profilometry (S Neox and SensoSCAN 6.3, Sensofar, Spain), where three samples from each test group were scanned with a green LED with an EPI 150X objective in the bright field mode at six random non-overlapping positions with a surface evaluation area of 116.96 μm × 88.06 μm (1360 px × 1024 px). Surface parameters were obtained from image analysis and processing (7.3 SensoMap Standard, Sensofar, Digital Surf's Mountains Technology®, Spain). The results are registered as the mean of three measurements performed. Profilometry measurements of the developed interfacial area ratio (Sdr) were performed with an optical profiler and controlled with a designated software. Sdr is the surface area ratio between a flat, "projected," surface and a textured, "developed," surface with an identical footprint (Sdr = 0 for a flat surface).

2.6. X-ray diffraction characterization

The crystal structures of one disc from each group were characterized by X-ray diffraction (XRD). A powder diffractometer (D8 Discover, Bruker AXS) in Bragg–Brentano configuration with a Ge(111) monochromator and a Lynxeye detector with $CuK_{\alpha 1}$ radiation was used. All samples were measured in the angular range of 2–100° with a step size of 0.02° and a counting time per step of 0.7 s. Rietveld analysis was carried out (TOPAS V5, Bruker AXS) in the angular range 16–98° [22]. The experimental data were fitted to the following structural models; $Y_{0.04}Zr_{0.96}O_{1.96}$ (space group (SG) = P42/nmc Z, ICSD = 62,994), $Y_{0.1}Zr_{0.9}O_{1.95}$ (SG = P42/nmc S, ICSD = 75,309), $Y_{0.214}Zr_{0.786}O_{1.893}$ (SG = Fm-3 m, ICSD = 165,036), ZrO_2 (SG = P121/c1, ICSD = 18,190). Thirty-three independent parameters were fitted for each dataset, using a 10 parameter background polynomial, fitting a simple axial model, sample height displacement, individual phase scale factors, with peak shapes fitted to a Gaussian function. In addition, the preferred orientation in the (1-1-1) direction was refined for the monoclinic (*m*) phase. Yttria content was obtained directly by parametric Rietveld refinement where equations presented by Lipkin et al. describing the yttria content as a function of the cell parameters were fitted [23,24].

2.7. Cementation of crowns

Copies of the original preparation were made from a dental composite material (SDR Flow+, Dentsply Sirona, Konstanz, Germany) produced in an impression mold (Affinis, Coltene/Whaledent Gmbh, Germany). These copies were used as abutment tooth substitutes. Cementation was performed according to producers' instruction (RelyX Unicem, 3M, USA). All crowns were cemented by the same procedure. After seating the crowns, a standardized 1500 g seating load was applied by a cementation jig. The cement was light-cured for 2 s from two sides, before excess cement was removed using a scalpel. Finally, they were light-cured for 20 s each from five directions. All specimens were kept dry at room temperature for 15 min following cementation and then immersed in 37 °C distilled water (24 ± 2 h).

2.8. Fracture testing

All the cemented crowns and discs were subjected to loading in a universal test machine (Zwick/Roell, Ulm, Germany) in circulating water at 37 °C until failure and load at fracture (N) was recorded and used for the analyses.

2.8.1. Crowns

Each abutment with a cemented crown was placed on a platform in circulating water of 37 °C and loaded by a spherical steel piston from the top of the crown with a rubber cushion in between to avoid contact damage at the crown surface, by using a crosshead speed (load rate) of 0.5 mm/min, the load was applied until fracture. The fracture loads were recorded and the pieces collected.

2.8.2. Discs

The thickness and diameter of all discs were measured before testing. All specimens were loaded until fracture according to 7.3.2 Biaxial flexural strength-test ISO 6872:2015 (piston-on-three-ball test). The treated surface of the specimens was placed under tension, positioned down against three supporting steel balls. Polyethylene sheets (0.05 mm thickness) were placed between the specimen and the supports and the loading piston during testing. A crosshead speed (load rate) of 1 mm/min was applied until fracture and fracture load (N) was recorded. The fracture fragments for each disc were captured and the number of fracture fragments was registered.

2.9. Fracture analyses

All crown specimens and two disc specimens from each group were analyzed by fractographic methods and crack origin and propagation were identified [25]. The fractured pieces were inspected by both light microscopy and scanning electron microscopy for fracture analyzes and cement retention. Fracture modes were compared to failure modes of similar restorations failed during clinical use.

2.10. Statistical analysis

Non-parametric statistics were used. For overall comparison Kruskal–Wallis test was used, with correction for multiple groups. Mann–Whitney U-test was used for comparison between groups. Spearman's rank test was used to assess correlations among variables. The level of significance was set to α = 0.05. The data were analyzed with a statistical software package (IBM SPSS statistics 25, Chicago, Ill, US).

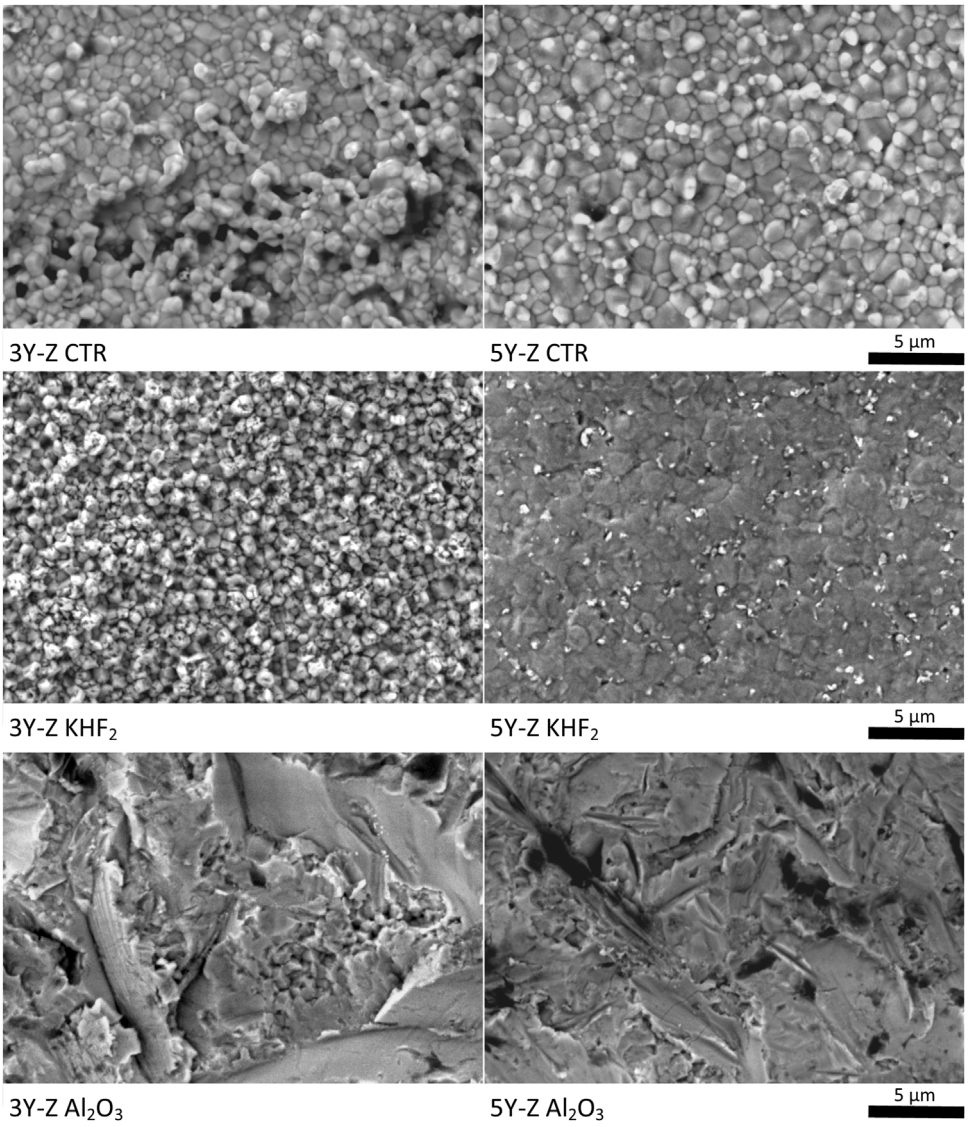

Fig. 2 – The surface structure in the different test groups as observed in the disc-shaped specimens. SEM was performed with BSE for all samples, black scale bar indicates 5 µm.

3. Results

There were differences between the tested materials in all the assessed variables. Furthermore, the effect of the pre-treatment differed between disc- and crown-shaped specimens.

3.1. *Crown margins*

All crowns had minor flaws, chips, or irregularities from the machining on the crown margins. One crown (5Y-Z) was excluded due to a margin flaw larger than 0.1 mm. This crown was replaced in order to achieve 30 specimens without major flaws in each group. Half of the crowns displayed minor areas on outside walls affected by the treatment of the intaglio surface observed as small areas with matted surface (2 of 20 Al_2O_3 and 18 of 20 KHF_2).

3.2. *Surface effect*

The surface roughness and surface morphology differed among the test groups (Figs. 2 and 3, Table 2). The effect of the KHF_2 differed between the crown- and disc-shaped specimens. The surfaces of the discs had a homogenous appearance as seen in Fig. 2, whereas the crowns showed a mixture of etched patches and pristine crown walls. The control specimens had areas with zircona particles appearing to be adhering to the surface (Figs. 2 and 4).

There was a statistically significant difference in wettability with water, but not with bonding liquid among the groups

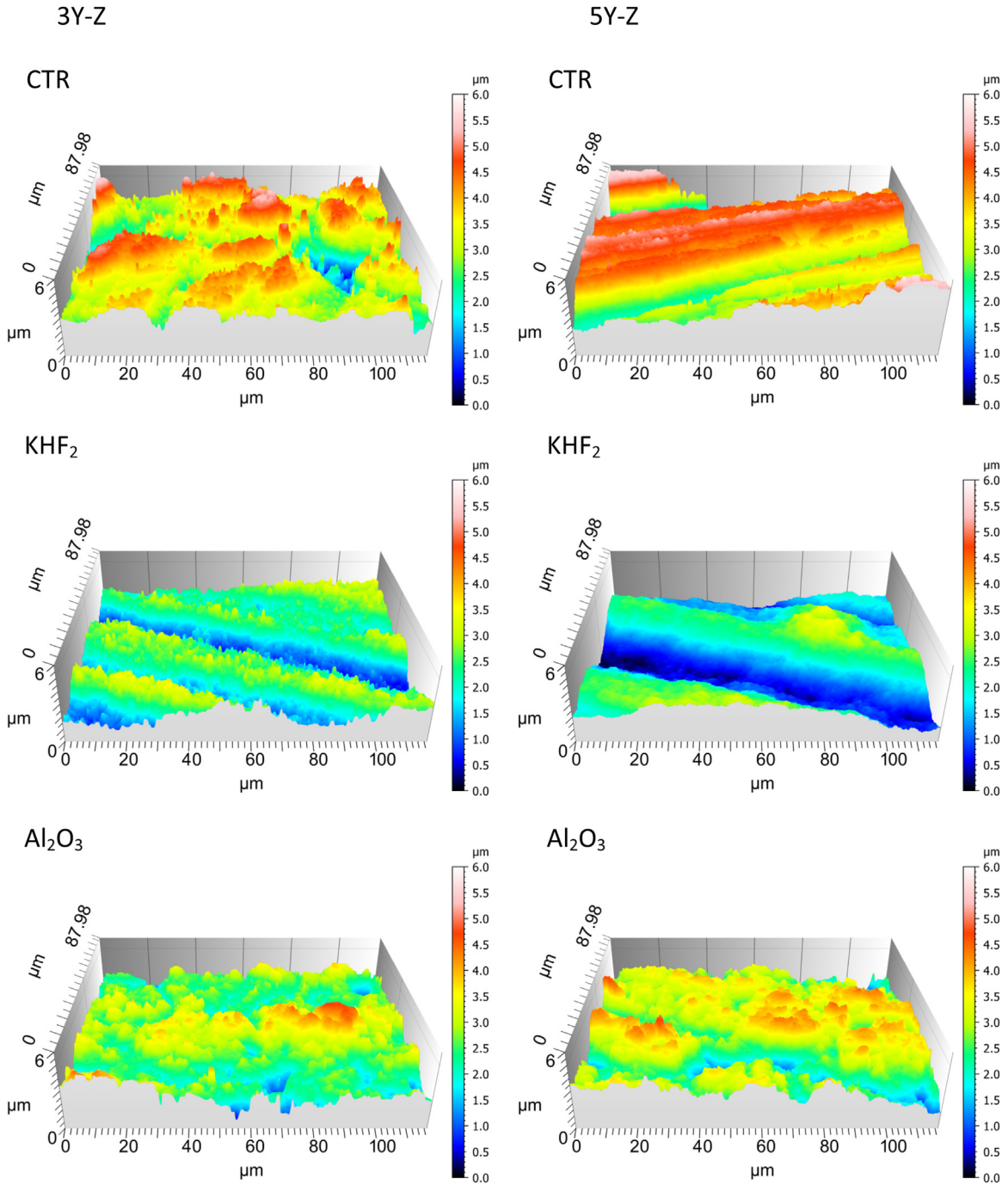

Fig. 3 – Images of the surface topography of the different test groups (discs) taken by a profilometry imaging technique.

Table 2 – Overview over the mean (standard deviation) of the measurements of surface properties of the disc-shaped specimens. Values marked with the same superscript letters in each row are not statistically significant different from each other.

	3Y-Z CTR	3Y-Z KHF_2	3Y-Z Al_2O_3	5Y-Z CTR	5Y-Z KHF_2	5Y-Z Al_2O_3
Contact angle; water (n = 10)*	60.1°(5)^a	16.3°(4)^b	82.2°(6)^c	54.7°(4)^a	7.2°(4)^d	79.8°(12)^c
Contact angle; bonding (n = 5)*	30.6°(3)^a	35.6°(2)^a	34.0°(5)^a	33.6°(1)^a	34.8°(1)^a	37.0°(3)^a
Sdr** (n = 3)*	11.3°(3.6)	8.3°(0.7)	10.3°(1.2)	4.6°(2.7)	1.4°(0.4)	8.4°(0.7)

* Number of specimens assessed per test group.
** Sdr: developed interfacial area ratio.

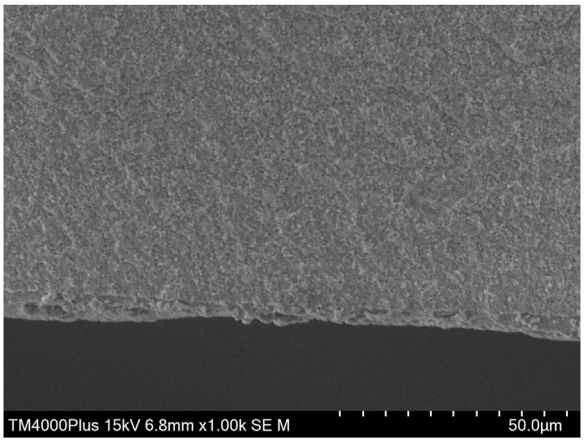

Fig. 4 – Secondary emission scanning electron image of a fractured disc specimen in the 3Y-Z control group revealing a thin layer of remaining machining dust on the tensile stress surface (bottom). This dust layer is partially sintered to the surface and creates a rough surface as can be observed in Fig. 2. SEM imaging was performed at 1000× magnification with SE detector. Scale is shown with 50 µm scale bar (white).

(Table 2). There were also considerable differences among the test groups in surface roughness as measured in Sdr.

3.3. *Strength*

There were statistically significant differences in load at fracture between test groups for both crown- and disc-shaped specimens (Fig. 5A and B).

3.4. *Fracture mode*

Fracture origin and crack propagation were found in all specimens, but the appearance of the origin differed between discs and crowns. The crown-shaped specimens fractured in mainly two different modes, from the crown margin's mesial or distal region or from the intaglio occlusal surface. The fracture mode of the discs revealed that fracture initiation was minor surface or subsurface flaws on the tensile stress side. Distinct fracture mirrors surrounded the fracture origins in the discs only. The discs fractured in 2–6 pieces. There was a positive correlation between fracture stress and number of fragments (Spearman's $r = 0.42$, $p < 0.001$).

3.4.1. *Cement retention*

Most of the crowns had some remaining cement on the intaglio walls, and in some cases, it was not possible to separate them from the composite abutment. The amount of remaining cement varied among groups (Figs. 6 and 7). There was a statistically significant correlation between load at fracture and the amount of cement retention (0.26, $p = 0.04$).

3.5. *Crystallographic characterization*

The amount of yttria as measured by X-ray diffraction (XRD) was 4.25 (range 3.22–6.23) for the 3Y-Z and 7. 47 (range 6.31–8.95) for the 5Y-Z The phase fractions of the cubic, monoclinic, and tetragonal phases for all samples analyzed with Rietveld refinement is shown in Table 3. The tetragonal phase was fitted to two tetragonal phases denoted t and t^1 as seen in Fig. 8 (ICDS = 62,994 and 75,309 respectively). The tetragonal phase is the sum of the phase fraction on t and t^1 and is the dominating phase for all samples. The tetragonal phase did, however, differ slightly between the controls and the Al_2O_3 (Fig. 8).

4. Discussion

The results revealed that the null hypotheses could be rejected. Both the amount of yttria-stabilizer and pre-cementation treatment affected load at fracture, surface roughness, cement retention and crystallographic composition. Neither of the pre-treatments resulted in a reduction of fracture resistance. The highest load at fracture was achieved by the air-abraded 3Y-Z (3Y-TZP) specimens, both disc- and crown-shaped. The finding that cement retention was higher on the intaglio crown walls on the pretreated compared to the untreated crowns indicates that an increased retentive effect of both etching with KHF_2 and air-abrasion with Al_2O_3 was obtained. It was not possible to ensure a conformal coating

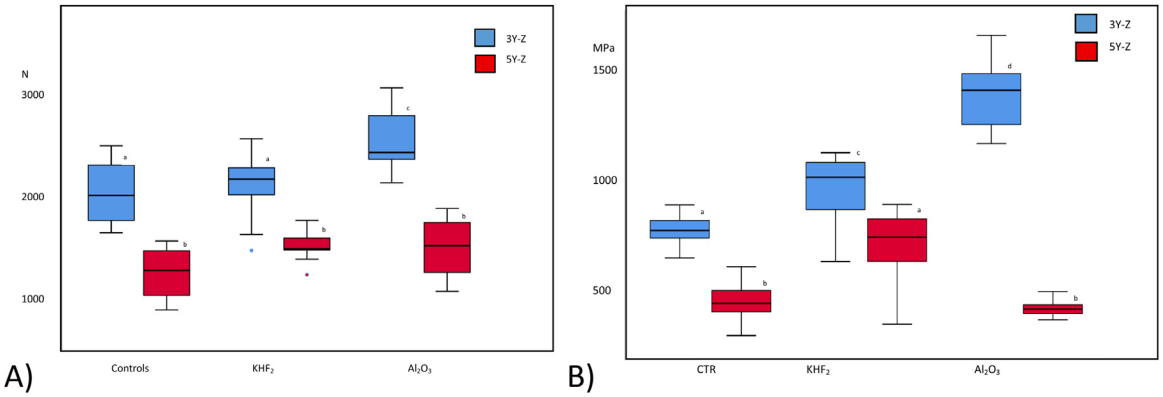

Fig. 5 – Boxplots of (A) the fracture loads [N] in the different test groups for the crown-shaped specimens in N and (B) fracture stress [MPa] the disc-shaped specimens in. Boxes marked with identical letters are not statistically significant from each other ($p > 0.05$). The boxes represent 75% of the values. The horizontal bars represent the median value.

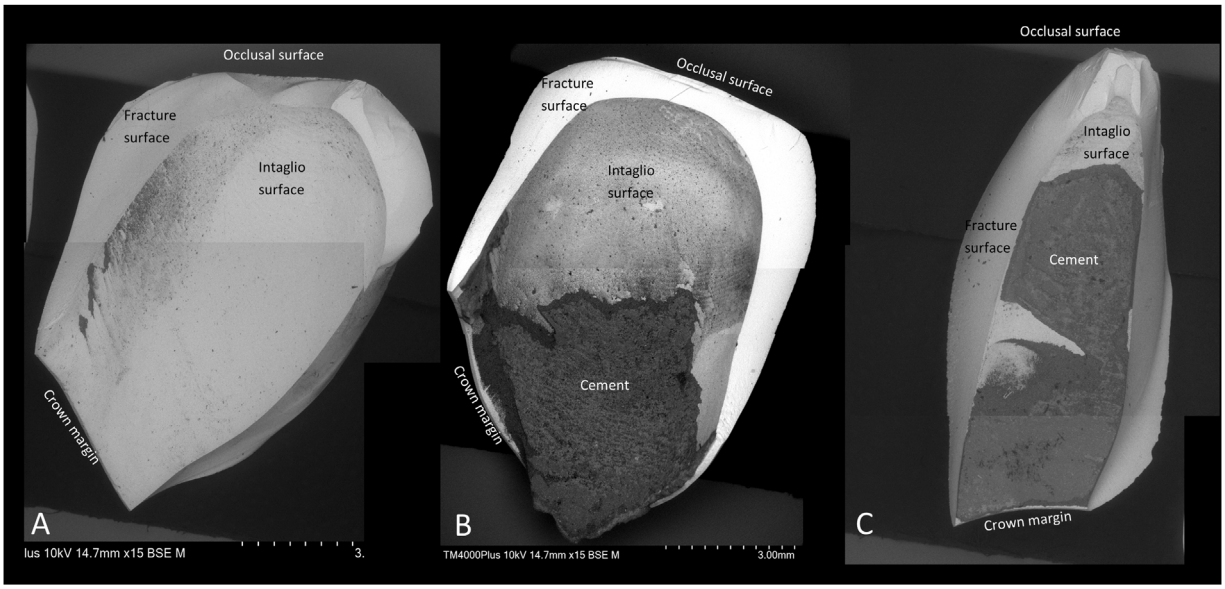

Fig. 6 – The amount of cement (dark) remaining on the intaglio walls after load testing varied greatly from (A) little to no cement, (B) large areas of cement to (C) mostly covered by cement. The fracture origins in crown A and C are the intaglio surface on the occlusal wall, while the origin in crown B is marginal. SEM imaging performed with BSE detector at 15× magnification.

of the etchant inside the crowns throughout the etching process. This resulted in effective etching only on localized areas on the intaglio axial walls.

4.1. *Margin quality*

There were no significant differences in margin quality between the standard 3Y-Z and the more translucent 5Y-Z crowns. In general, the margin quality was high with the exception of one 5Y-Z crown which was excluded due to a large margin defect. This defect was most likely due to faulty manufacturing. Previous studies reveal that there are large discrepancies in the severity of machining defects among dental ceramics [26–29]. The present findings indicate that the tested materials machined with the producers' own milling unit does not generate severe machining defects. The pre-treatment did affect the crown margins as some surface changes could be observed on the outside of the crown walls as areas with matt surface. These effects were especially prominent on the etched crowns revealing the difficulty in containing the liquid inside a cap-shape without a levelled rim. This could perhaps be solved by using KHF_2 in a gel-like solution instead of a dry powder.

4.2. *Surface effects*

SEM imaging showed identifiable crystallites on the surface of the as-sintered CTR samples as expected. Grains of zirconia was, however, observed on the sample surface, including multiple undercuts, for both disc- and crown-shaped samples. These grains resulted in a surprisingly rough surface as seen in Fig. 4. The attached zirconia particles observed in the SEM are probably due to zirconia dust remaining on the sample surface after the machining/milling process which is sintered to the bulk sample during the subsequent sintering process. The amount of cement retained on the intaglio walls of the crown revealed, however, that the untreated controls had less retentive effect than the two other surface treatments, despite the appearance and relatively high surface roughness. It is possible that some superficial grains were pulled off the surface with the cement during loading. The results indicate, however, that removal of machining dust must be performed with care in order to secure optimal fit and cement flow.

The surface structures of the etched specimens were visibly different in SEM compared to CTR-samples for both discs and crowns as seen in Figs. 2 and 6. The 3Y-Z KHF_2 displayed increased tortuosity and a more "pop-corn"-like surface compared to the controls. The 5Y-Z KHF_2, on the other hand, seemed to be smoothened compared to the controls. The surface roughness evaluations (Sdr) confirm this observation.

Table 3 – Phase fractions and yttria-content from Rietveld analysis of control (CTR), etched (KHF_2), and sandblasted (Al_2O_3) of Prettau zirconia (3Y-Z) and Prettau anterior (5Y-Z). The tetragonal phase content is the sum of the two t-phases (t + t′).

	Phase fraction		
	Tetragonal	Monoclinic	Cubic
3Y-Z CTR	91	6	3
3Y-Z KHF_2	87	10	3
3Y-Z Al_2O_3	56	7	37
5Y-Z CTR*	77	0	23
5Y-Z KHF_2	92	1	7
5Y-Z Al_2O_3	85	0	15

* The yttria amount in 5Y-Z CTR is overestimated due to anisotropic peak broadening (see Fig. 8).

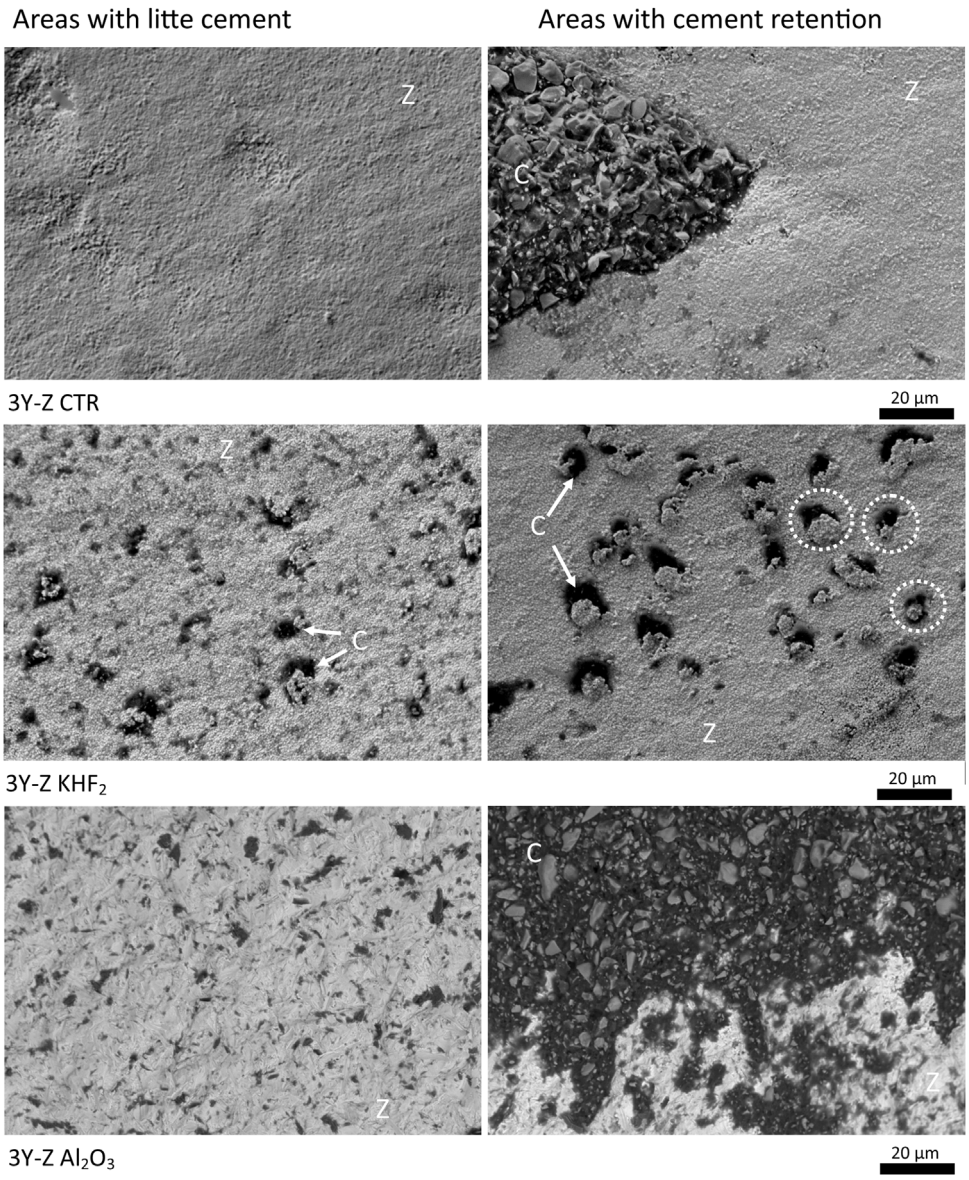

Fig. 7 – Examples of the differences in cement retention on the crown walls on the 3Y-Z test group. The zirconia(z) is bright, and the cement (c) is dark. Note the patched effect of the hot etching on the crown walls in the 3Y-Z KHF_2 group (dotted circles). SEM imaging performed with BSE detector. Black scale bar indicates 20 µm.

Both surface roughness and surface energy may affect the wettability of a material as shown in previous studies as well [30,31]. The different treatments greatly affected the wettability by deionized water, but not the tested bonding material. The KHF_2 etching increased the surface energy and the Al_2O_3 air-abrasion reduced the surface energy compared with the untreated control surfaces for both materials. This indicates that air-abrasion should be less beneficial for cement wetting than acid etching, although the same effect could not be observed for the bonding material used. Previous studied have, however, found that air abrasion increased wettability and further studies are necessary to fully understand the effects on adhesive materials [31]. The finding that the air-abraded crowns had the highest degree of cement retention and that there were no differences in contact angle of a resin droplet among the groups supports that the surface energy was sufficient for good wetting of polymer-based cement [30].

The monoclinic phase fraction remained relatively unchanged for all 3Y-Z samples, meaning that the high cubic phase fraction of the 3Y-Z Al_2O_3 sample is caused by a phase transition from tetragonal to cubic phase caused by the air-abrasion. Normally a *t-m* transformation is observed in zirconias subjected to surface stress for 3Y-Z [32,33]. The present finding of increased cubic phase and reduction of monoclinic phase is, however also shown in some studies [33–35]. The explanation might be a reverse transformation process. It should be noted that Rietveld refinement was demanding for the sandblasted samples. This is probably caused by the highly strained crystallites at the surface of the air-abraded samples, resulting in anisotropic peak broadening in the XRD

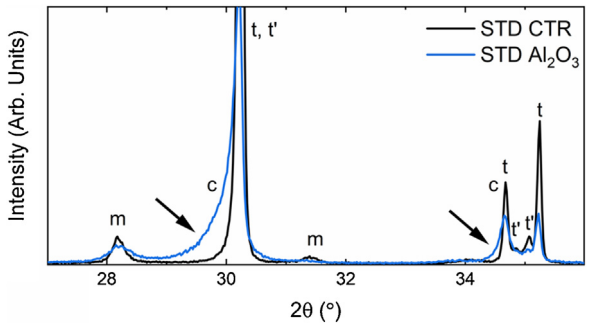

Fig. 8 – X-ray diffractograms of 3Y-Z CTR and 3Y-Z Al_2O_3 samples. c, m, t′ and t denote reflections from the cubic, monoclinic and two tetragonal phases (t′ and t). Arrows indicate the effect of anisotropic peak broadening. Measured with Cu $K\alpha_1$ radiation.

for these samples. An example of this broadening is shown in Fig. 8, highlighted with arrows, where the 3Y-Z CTR had symmetric reflections and 3Y-Z Al_2O_3 showed considerable asymmetry of the reflections (Fig. 8). This has most likely resulted in an overestimation of the Y_2O_3 content in the 3Y-Z Al_2O_3 sample.

For all 5Y-Z samples the amount of monoclinic phase fraction was 0–1%, in contrast to the 3Y-Z with a monoclinic phase fraction of 6–10%. The difference in phase fractions is to be expected from the different amounts of the yttria-stabilizer [33]. Both 5Y-Z CTR and 5Y-Z Al_2O_3 samples had a considerable amount of cubic phase, 23 and 15%, respectively, compared to only 7% cubic phase fraction in the 5Y-Z KHF_2 sample. In the case of 3Y-Z CTR and 3Y-Z KHF_2 only a minor difference in cubic phase fraction was detected compared to the significant difference in cubic phase fraction between 5Y-Z CTR and 5Y-Z KHF_2.

The reduction in cubic phase content for 5Y-Z KHF_2 was most likely caused by the removal (by etching) of surface material with a higher cubic phase content compared to the bulk of the sample.

4.3. *Strength*

Fracture strength was improved by both air-abrasion and etching compared to the control samples for the zirconia with low yttria-content (3Y-Z) in both disc- and crown-shaped specimens. This is in accordance with previous studies [16,36]. As expected from the Y_2O_3–ZrO_2 phase diagram, we observed a higher cubic phase content for the 5Y-Z compared to the 3Y-Z CTR sample [37]. We also observed a considerable amount of the monoclinic phase for all 3Y-Z samples (6–10%), whereas we only observed ~1% monoclinic phase for the 5Y-Z KHF_2 samples (no monoclinic phase detected for 5Y-Z CTR and 5Y-Z Al_2O_3). In the case of the 5Y-Z samples, we observed an increase in strength for the etched samples. However, in the case of 5Y-Z Al_2O_3 there was a tendency towards reduction in strength. This was in contrast to the 3Y-Z samples where both air-abrasion and etching resulted in increased fracture strength, with air-abrasion the most (Fig. 4B).

Increased strength was observed for the 5Y-Z KHF2 compared to the controls and the air-abraded 5Y-Z group. The increased strength can be related to a reduction in the cubic phase. The importance of the *t-m* phase transition has widely been associated with the high strength of zirconia [16,32]. The cubic phase is more prone to crack initiation, and a surface with a high cubic content is more prone to cracking [20,38]. Removing the surface layer with high cubic phase content in favor of a new surface with a higher amount of tetragonal phase is expected to increase the flexure strength. This is somewhat contradictory to the observed high cubic content on the surface of the 3Y-Z Al_2O_3, with this resulting in the highest measured flexure strength. However, the observed differences in strength caused by different surface treatments indicate the more fundamental differences between 3Y and 5Y zirconia materials. Further studies should, in more depth, investigate the fundamental differences occurring when varying the yttria content in zirconia for dental applications. Our results from the studies of 3Y-Z and 5Y-Z materials shed light on the surface treatment of dental zirconia and the importance of optimizing the treatment procedure to the specific yttria content. Furthermore, the present study only assessed the immediate effect of the different pre-cementation procedures. How the surface treatments affect long-term aging of zirconia and cement retention is thus uncertain.

4.4. *Cement retention*

Previous studies indicate a relationship between crown strength and bonding between tooth-cement and crown [38] while others do not find this effect for zirconia-based crowns [39]. The finding that the relative relationship in strength among the test groups is similar for discs and cemented crowns indicate that increased retention does not affect material strength. Increased retention is, however, critical in order to reduce the risk of crown loosening. The significant increase of cement retained inside the fractured crowns compared to the untreated controls indicated that both pre-cementation procedures improve cement retention.

4.5. *Fracture mode*

The finding that none of the crowns fractured from contact damages, but displayed fracture modes similar to those observed in clinical failures [40–45] even though the loads at fracture are somewhat higher than human mastication forces. It must be taken into consideration that dental restorations are subjected to multiple and repetitive forces during clinical function, whereas in the present study quasi-static force is used for provoking the fractures. Nevertheless, the similarity between clinical fractures and the fractures observed in this study indicated that the current test method is more clinically relevant than fracture strength tests creating contact damages at the loading site [46–49]. The fracture origins differed between the crown and the discs. Fracture mirrors as seen in all the discs were not readily observed in the crown-shaped specimens.

5. Conclusion

Pre-cementation procedures affected the load at fracture and cement retention in dental zirconias. Air-abrasion resulted in the highest strength for zirconia with moderate yttria content (<4 mol%/3Y). Acid etching with heated KHF_2 seemed to have the best effect on strength and cement retention on zirconias with higher yttria content (>5 mol%/5Y). The application was, however, complicated. Air abrasion with Al_2O_3 should be used with caution for pre-treating zirconia with higher yttria content (>5 mol%), as it has possible negative effects on strength. Pre-cementation procedures need to be adjusted for the different dental zirconia materials to optimize both strength and retention.

REFERENCES

[1] Passia N, Mitsias M, Lehmann F, Kern M. Bond strength of a new generation of universal bonding systems to zirconia ceramic. J Mech Behav Biomed Mater 2016;62:268–74.
[2] Kern M, Wegner SM. Bonding to zirconia ceramic: adhesion methods and their durability. Dent Mater 1998;14:64–71.
[3] Inokoshi M, De Munck J, Minakuchi S, Van Meerbeek B. Meta-analysis of bonding effectiveness to zirconia ceramics. J Dent Res 2014;93:329–34.
[4] Martins FV, Mattos CT, Cordeiro WJB, Fonseca EM. Evaluation of zirconia surface roughness after aluminum oxide airborne-particle abrasion and the erbium-YAG, neodymium-doped YAG, or CO_2 lasers: a systematic review and meta-analysis. J Prosthet Dent 2019;121:895–903.e2.
[5] Hallmann L, Ulmer P, Lehmann F, Wille S, Polonskyi O, Johannes M, et al. Effect of surface modifications on the bond strength of zirconia ceramic with resin cement resin. Dent Mater 2016;32:631–9.
[6] Kern M, Passia N, Sasse M, Yazigi C. Ten-year outcome of zirconia ceramic cantilever resin-bonded fixed dental prostheses and the influence of the reasons for missing incisors. J Dent 2017;65:51–5.
[7] Kern M. Bonding to oxide ceramics—laboratory testing versus clinical outcome. Dent Mater 2015;31:8–14.
[8] Shahin R, Kern M. Effect of air-abrasion on the retention of zirconia ceramic crowns luted with different cements before and after artificial aging. Dent Mater 2010;26:922–8.
[9] Aung SSMP, Takagaki T, Lyann SK, Ikeda M, Inokoshi M, Sadr A, et al. Effects of alumina-blasting pressure on the bonding to super/ultra-translucent zirconia. Dent Mater 2019;35:730–9.
[10] Sriamporn T, Thamronganankul N, Busabok C, Poolthong S, Uo M, Tagami J. Dental zirconia can be etched by hydrofluoric acid. Dent Mater J 2014;33:79–85.
[11] Smielak B, Klimek L. Effect of hydrofluoric acid concentration and etching duration on select surface roughness parameters for zirconia. J Prosthet Dent 2015;113:596–602.
[12] Le M, Larsson C, Papia E. Bond strength between MDP-based cement and translucent zirconia. Dent Mater J 2019;38:480–9.
[13] Ruyter EI, Vajeeston N, Knarvang T, Kvam K. A novel etching technique for surface treatment of zirconia ceramics to improve adhesion of resin-based luting cements. Acta Biomater Odontol Scand 2017;3:36–46.
[14] Sagen MA, Kvam K, Ruyter EI, Rønold HJ. Debonding mechanism of zirconia and lithium disilicate resin cemented to dentin. Acta Biomater Odontol Scand 2019;5:22–9.
[15] Armstrong S, Breschi L, Özcan M, Pfefferkorn F, Ferrari M, Van Meerbeek B. Academy of Dental Materials guidance on in vitro testing of dental composite bonding effectiveness to dentin/enamel using micro-tensile bond strength (muTBS) approach. Dent Mater 2017;33:133–43.
[16] Botelho MG, Dangay S, Shih K, Lam WYH. The effect of surface treatments on dental zirconia: an analysis of biaxial flexural strength, surface roughness and phase transformation. J Dent 2018;75:65–73.
[17] Wang H, Aboushelib MN, Feilzer AJ. Strength influencing variables on CAD/CAM zirconia frameworks. Dent Mater 2008;24:633–8.
[18] Kvam K, Irkayek A, Vangaeva E, El-Homsi F. Comparison of sandblasted, ground and melt-etched zirconia crowns regarding adhesion strength to resin cement. Biomater Investig Dent 2019;6:1–5.
[19] Hooi P, Addison O, Fleming GJ. Strength determination of brittle materials as curved monolithic structures. J Dent Res 2014;93:412–6.
[20] Zhang Y. Making yttria-stabilized tetragonal zirconia translucent. Dent Mater 2014;30:1195–203.
[21] Yan J, Kaizer MR, Zhang Y. Load-bearing capacity of lithium disilicate and ultra-translucent zirconias. J Mech Behav Biomed Mater 2018;88:170–5.
[22] Bruker A. Topas V4. 2: General profile and structure analysis software for powder diffraction data. Karlsruhe, Germany: Bruker AXS; 2009. Karlsruhe, Germany: Bruker AXK; 2009.
[23] Lipkin DM, Krogstad JA, Gao Y, Johnson CA, Nelson WA, Levi CG. Phase evolution upon aging of air-plasma sprayed t′-zirconia coatings: I—synchrotron X-ray diffraction. J Am Ceram Soc 2013;96:290–8.
[24] Stinton GW, Evans JSO. Parametric Rietveld refinement. J Appl Crystallogr 2007;40:87–95.
[25] 1322-02 AC. Standard practice for fractography and characterization of fracture origins in advances ceramics. Annual book of ASTM standards. West conshocken, PA, Philadelphia: American Society for Testing and Materials; 2002.
[26] Schriwer C, Skjold A, Gjerdet NR, Øilo M. Monolithic zirconia dental crowns. Internal fit, margin quality, fracture mode and load at fracture. Dent Mater 2017;33:1012–20.
[27] Denry I, Kelly JR. State of the art of zirconia for dental applications. Dent Mater 2008;24:299–307.
[28] Rekow D, Thompson VP. Near-surface damage—a persistent problem in crowns obtained by computer-aided design and manufacturing. Proc Inst Mech Eng 2005;219:233–43.
[29] Luthardt RG, Holzhüter MS, Rudolph H, Herold V, Walter MH. CAD/CAM-machining effects on Y-TZP zirconia. Dent Mater 2004;20:655–62.
[30] Strasser T, Preis V, Behr M, Rosentritt M. Roughness, surface energy, and superficial damages of CAD/CAM materials after surface treatment. Clin Oral Investig 2018;22:2787–97.
[31] Alagiriswamy G, Krishnan CS, Ramakrishnan H, Jayakrishnakumar SK, Mahadevan V, Azhagarasan NS. Surface characteristics and bioactivity of zirconia (Y-TZP) with different surface treatments. J Pharm Bioallied Sci 2020;12:S114–23.
[32] Bergamo E, da Silva WJ, Cesar PF, Del Bel Cury AA. Fracture load and phase transformation of monolithic zirconia crowns submitted to different aging protocols. Oper Dent 2016;41:E118–30.
[33] de Araújo-Júnior ENS, Bergamo ETP, Campos TMB, Benalcázar Jalkh EB, Lopes ACO, Monteiro KN, et al. Hydrothermal degradation methods affect the properties and phase transformation depth of translucent zirconia. J Mech Behav Biomed Mater 2020;112:104021.
[34] Vila-Nova TEL, Gurgel de Carvalho IH, Moura DMD, Batista AUD, Zhang Y, Paskocimas CA, et al. Effect of

finishing/polishing techniques and low temperature degradation on the surface topography, phase transformation and flexural strength of ultra-translucent ZrO_2 ceramic. Dent Mater 2020;36:e126–39.
[35] Skienhe H, Habchi R, Ounsi H, Ferrari M, Salameh Z. Evaluation of the effect of different types of abrasive surface treatment before and after zirconia sintering on its structural composition and bond strength with resin cement. Biomed Res Int 2018;2018, 1803425-.
[36] Amaral M, Cesar PF, Bottino MA, Lohbauer U, Valandro LF. Fatigue behavior of Y-TZP ceramic after surface treatments. J Mech Behav Biomed Mater 2016;57:149–56.
[37] Krogstad JA, Leckie RM, Kramer S, Cairney JM, Lipkin DM, Johnson CA, et al. Phase evolution upon aging of air-plasma sprayed t′-zirconia coatings: II—Microstructure evolution. J Am Ceram Soc 2013;96:299–307, http://dx.doi.org/10.1111/j.1551-2916.2012.05460.x.
[38] Lawson NC, Jurado CA, Huang CT, Morris GP, Burgess JO, Liu PR, et al. Effect of surface treatment and cement on fracture load of traditional zirconia (3Y), translucent zirconia (5Y), and lithium disilicate crowns. J Prosthodont 2019;28:659–65.
[39] Nakamura K, Mouhat M, Nergard JM, Laegreid SJ, Kanno T, Milleding P, et al. Effect of cements on fracture resistance of monolithic zirconia crowns. Acta Biomater Odontol Scand 2016;2:12–9.
[40] Øilo M, Quinn GD. Fracture origins in twenty-two dental alumina crowns. J Mech Behav Biomed Mater 2016;53:93–103.
[41] Pang Z, Chughtai A, Sailer I, Zhang Y. A fractographic study of clinically retrieved zirconia–ceramic and metal–ceramic fixed dental prostheses. Dent Mater 2015;31:1198–206.
[42] Øilo M, Hardang AD, Ulsund AH, Gjerdet NR. Fractographic features of glass-ceramic and zirconia-based dental restorations fractured during clinical function. Eur J Oral Sci 2014;122:238–44.
[43] Quinn GD, Hoffman K, Scherrer S, Lohbauer U, Amberger G, Karl M, et al. Fractographic analysis of broken ceramic dental restorations. Fractography of glasses and ceramics VI. John Wiley & Sons, Inc.; 2012. p. 161–74.
[44] Øilo M, Kvam K, Gjerdet NR. Load at fracture of monolithic and bilayered zirconia crowns with and without a cervical zirconia collar. J Proshtet Dent 2016;115:630–6.
[45] Hansen TL, Schriwer C, Øilo M, Gjengedal H. Monolithic zirconia crowns in the aesthetic zone in heavy grinders with severe tooth wear—an observational case-series. J Dent 2018;72:14–20.
[46] Kelly JR, Benetti P, Rungruanganunt P, Bona AD. The slippery slope: critical perspectives on in vitro research methodologies. Dent Mater 2012;28:41–51.
[47] Anusavice KJ, Kakar K, Ferree N. Which mechanical and physical testing methods are relevant for predicting the clinical performance of ceramic-based dental prostheses? Clin Oral Implants Res 2007;18:218–31.
[48] Øilo M, Kvam K, Tibballs JE, Gjerdet NR. Clinically relevant fracture testing of all-ceramic crowns. Dent Mater 2013;29:815–23.
[49] Aboushelib MN, Feilzer AJ, Kleverlaan CJ. Bridging the gap between clinical failure and laboratory fracture strength tests using a fractographic approach. Dent Mater 2009;25:383–91.